

### Alexandria Journal of Science and Technology



Article

# On the Fractional Wiener Process and Some Stochastic Epidemic Models

Khairia El-Said El-Nadi, Mohamed El-Shindidy, Aleya Abdelghany Lashen\*

Department of Mathematics and Computer Science, Faculty of Science, Alexandria University, Egypt.

\* Correspondence Address:

Aleya Abdelghany Lashen: Department of Mathematics and Computer Science, Faculty of Science, Alexandria University, Egypt. Email: aleya.abdelghany@gmail.com.

**KEYWORDS:** Wiener Process; Fractional stochastic models; Stochastic integral epidemic model; SIR epidemic modeling; Fractional calculus; Probabilistic epidemic dynamics.

Received:
June 21, 2025
Accepted:
August 26, 2025
Published:
October 18, 2025

ABSTRACT: This study develops a fractional stochastic framework for modeling epidemic spread, based on a recently proposed fractional Wiener process. The proposed model generalizes the classical SIR structure by incorporating fractional Brownian motion, which captures memory effects and long-range dependencies observed in real-world epidemiological data. The system is formulated through stochastic differential equations, using Itô stochastic calculus with fractional methods to describe transmission dynamics under uncertainty. The analysis addresses existence, uniqueness, and qualitative properties of the solutions to the fractional stochastic model. Numerical simulations are conducted to demonstrate the system's behavior under various conditions and to illustrate the role of stochastic fluctuations in epidemic progression. A variant of the model using a fractional Ornstein–Uhlenbeck process is also considered to assess the influence of damping and noise. The results highlight the effectiveness of the proposed framework in capturing complex epidemic behaviors and provide a mathematically robust approach for analyzing disease transmission. This work offers valuable insights for researchers and contributes to the broader development of stochastic modeling in epidemiology.

# 1. INTRODUCTION

Modeling the spread of epidemics under uncertainty remains a central challenge in mathematical epidemiology. Traditional deterministic models, while useful for capturing general trends, often fail to account for the inherent randomness and memory-dependent dynamics observed in real-world outbreaks. These limitations may lead to oversimplified representations that do not reflect the complex, time-dependent interactions among individuals and their environments.

In recent years, fractional-order models have proved effective in capturing the memory and hereditary characteristics observed in epidemic dynamics. Although the present study does not adopt Caputo-type derivatives, such formulations have been successfully applied in several epidemic contexts, particularly in modeling COVID-19 transmission dynamics [1]. Fractional stochastic differential equations have emerged as powerful tools for integrating stochastic fluctuations with long-range temporal dependencies. These models simultaneously capture the randomness of disease transmission and the memory effects inherent in biological and social systems. Consequently, they offer a robust framework for analyzing and forecasting epidemic

behavior under uncertainty. This study introduces a fractional stochastic model grounded in the fractional Wiener process developed by El-Borai and El-Nadi [2-9], which generalizes classical Brownian motion by incorporating memory effects. The model is formulated using stochastic differential equations with fractional integrals and implemented within a generalized SIR framework to investigate epidemic dynamics.

The study investigates the probabilistic properties of the proposed system by analyzing the existence, uniqueness, and asymptotic stability of its solutions. Numerical simulations are presented to illustrate the impact of varying the basic reproduction number  $R_0$  on the epidemic peak and overall disease spread. Furthermore, an extended version of the model incorporating a fractional Ornstein–Uhlenbeck process is considered to assess the impact of damping and stochastic fluctuations [10].

By integrating advanced stochastic calculus with fractionalorder dynamics, this study presents a comprehensive modeling framework that captures both randomness and memory effects in disease transmission. This integrated approach enhances the understanding of epidemic progression under uncertainty and offers valuable insights for informing effective control strategies.

Fractional calculus extends classical differentiation and integration to non-integer orders, allowing mathematical models to incorporate memory and hereditary characteristics in a mathematically consistent manner. This approach is particularly valuable in epidemiology, where the present state of disease dynamics is often influenced by historical behavior. Fractional derivatives are especially effective in representing long-term temporal dependencies and non-local interactions in epidemic processes [11].

Stochastic integrals, particularly those driven by the Wiener (Brownian) process, offer a powerful approach for modeling the random fluctuations and uncertainties inherent in real-world epidemics. These uncertainties may arise from variability in human behavior, environmental conditions, and the implementation of public health measures [12]. When combined with fractional calculus, these tools provide a robust framework that captures both memory effects and stochastic disturbances. This integrated approach yields more realistic representations of epidemic dynamics compared to purely deterministic or classical stochastic models [13].

# 2. Fractional Stochastic System

To facilitate the understanding of the following model, we provide the definitions of the main variables and parameters used throughout the formulation:

S(t): Number of susceptible individuals at time t.

I(t): Number of infected individuals at time t.

R(t): Number of recovered individuals at time t.

 $\beta$ : Transmission rate from susceptible to infected individuals.

 $\gamma$ : Recovery rate of infected individuals.

 $R_0$ : Basic reproduction number.

 $\alpha$ : Order of the fractional derivative  $0 < \alpha \le 1$ .

 $\sigma_1$ : Volatility of the susceptible population S(t).

 $\sigma_2$ : Volatility of the infected population I(t).

b: The rate of birth from the infected to the susceptible state.

W(t): Standard Wiener process (Brownian motion), used to model stochastic fluctuations as the integral of Gaussian white noise.

Consider the following fractional stochastic system:

$$\begin{split} S(t) &= S(0) + \frac{1}{\Gamma(\alpha)} \int_0^t (t - \theta)^{\alpha - 1} \left[ -\frac{\beta}{N} S(\theta) + I(\theta) b \left( I(\theta) + R(\theta) \right) \right] d\theta + \frac{\sigma_1}{\Gamma(\alpha)} \int_0^t (t - \theta)^{\alpha - 1} S(\theta) dW(\theta), \end{split}$$

$$\begin{split} I(t) &= I(0) + \frac{1}{\Gamma(\alpha)} \int_0^t (t - \theta)^{\alpha - 1} \left[ \frac{\beta}{N} S(\theta) I(\theta) - I(\gamma + b) \right] d\theta + \frac{\sigma_2}{\Gamma(\alpha)} \int_0^t (t - \theta)^{\alpha - 1} I(\theta) dW(\theta), \end{split}$$

$$R(t) = R(0) + \frac{1}{\Gamma(\alpha)} \int_0^t (t - \theta)^{\alpha - 1} \left[ \gamma I(\theta) - bR(\theta) \right] d\theta - \frac{1}{\Gamma(\alpha)} \int_0^t (t - \theta)^{\alpha - 1} \left[ \sigma_1 S(\theta) + \sigma_2 I(\theta) \right] dW(\theta). \tag{2.1}$$

The proposed fractional stochastic system extends the classical SIR model by incorporating random effects through a fractional Wiener process. This formulation introduces memory into the transmission dynamics, capturing long-range dependence often observed in epidemic processes. While

comparable fractional stochastic methodologies have been applied to other epidemic frameworks, including extended forms such as the SIRS model [13], the present study focuses specifically on the fractional stochastic SIR framework to provide a clear and tractable analysis.

The following assumptions are made:

- a) S(0) > 0, I(0) > 0 and R(0) > 0.
- b) Population size *N* is constant and equal to the sum of individuals in three classes.
- c) The ratio between birth and death is one.
- d) The rate of moving directly from the infectious state to the susceptible state is equal to that from the recovered to susceptible states.

While this assumption simplifies the analysis, future extensions may consider time-varying population dynamics.

The classical SIR model and the fractional stochastic SIR model represent two distinct methodologies for simulating infection diseases. While the classical SIR model relies on deterministic parameters and has been foundational in epidemiological modeling, it lacks the flexibility to reflect real-world variability in transmission rates. In contrast, the fractional stochastic SIR model integrates both fractional calculus and stochastic elements, offering a more nuanced representation of disease spread by capturing memory effects and randomness.

Operating under a deterministic framework, the classical model assumes fixed transition rates between the Susceptible, Infected, and Recovered compartments. This rigidity limits its ability to respond to dynamic changes in the effective reproduction number observed in real outbreaks [14]. In contrast, the fractional stochastic SIR model extends this framework by incorporating fractional derivatives, which capture memory effects and allow past states to influence current dynamics [15]. By introducing stochasticity, it also accounts for inherent randomness and uncertainty in infection patterns [16].

Empirical findings indicate that the fractional stochastic model often yields lower root mean square errors compared to the classical formulation, particularly when the fractional order lies between 0.93 and 0.99 [16]. Although the model is computationally more demanding, it provides a flexible and realistic framework for understanding epidemic dynamics and capturing the complexity of epidemic processes, although it may pose additional challenges in calibration and interpretability.

## 3. Stochastic Integral Epidemic Model

The general model is presented in integral form, which naturally arises in the context of fractional calculus. However, for the special case when  $\alpha=1$ , the model is expressed in its equivalent differential form for clarity and analytical convenience.

Consider the case when  $\alpha = 1$ :

$$S(t) = S(0) + \int_0^t \left[ -\frac{\beta}{N} S(\theta) + I(\theta) b(I(\theta) + R(\theta)) \right] d\theta + \sigma_1 S(\theta) dW(\theta),$$

$$I(t) = I(0) + \int_0^t \left[ \frac{\beta}{N} S(\theta) I(\theta) - I(\gamma + b) \right] d\theta$$
$$+ \sigma_2 \int_0^t I(\theta) dW(\theta),$$

$$R(t) = R(0) + \int_0^t [\gamma I(\theta) - bR(\theta)] d\theta - \int_0^t [\sigma_1 S(\theta) + \sigma_2 I(\theta)] dW(\theta).$$
(3.1)

It can be observed that

$$S(t) + I(t) + R(t) = N = S(0) + I(0) + R(0),$$

This relation has been studied in several works, see [17-20].

Theorem 1. If  $\beta < \gamma + b$ , then:

$$\lim_{t\to\infty} E[I(t)] = \lim_{t\to\infty} E(R(t)) = 0, \quad \lim_{t\to\infty} E(S(t)) = N$$

Proof: Consider the equation

$$v(t) = I(0) + \int_0^t (\beta - \gamma - b)v(\theta)d\theta + \sigma_2 \int_0^t v(\theta)dW(\theta).$$

Consider the following stochastic differential equation,

$$dX(t) = \left[\frac{\sigma_2^2}{2} - (\beta - \gamma - b)\right] X(t) dt - \sigma_2 X(t) dW(t),$$
  
$$dY(t) = \left[\frac{\sigma_2^2}{2} + (\beta - \gamma - b)\right] Y(t) dt + \sigma_2 Y(t) dW(t),$$

The solution of these equations is given by

$$X(t) = e^{-\sigma_2 w(t) - (\beta - \gamma - b)t}$$
$$Y(t) = e^{\sigma_2 w(t) + (\beta - \gamma - b)t}$$

Set 
$$v^*(t) = X(t)v(t)$$

$$dv^{*}(t) = X(t)dv(t) + v(t)dX(t) + G_{1}(t)G_{2}(t)dt$$

$$= X(t) \left[ \left( (\beta - \gamma - b)t \right)v(t)dt + \sigma_{2}v(t)dw(\theta) \right] + v(t) \left[ \frac{\sigma_{2}^{2}}{2} - (\beta - \gamma - b) \right]X(t)dt - \sigma_{2}X(t)dw(t) - \sigma_{2}^{2}v(t)X(t)dt$$

$$dv^* = -\frac{\sigma_2^2}{2} dt, v^*(t) = e^{-\frac{\sigma_2^2}{2}t} I(0),$$

$$v(t) = Y(t)e^{-\frac{\sigma_2^2}{2}t} I(0) = e^{\sigma_2 W(t) + (\beta - \gamma - b)t} e^{-\frac{\sigma_2^2}{2}t} I(0),$$

$$E[v(t)] = e^{(\beta - \gamma - b)t} I(0)$$

Thus  $\lim_{t \to \infty} E[I(t)] = 0$ 

It can be observed that

$$E[R(t)] = R(0) + \gamma \int_0^t E[I(\theta)]d\theta - b \int_0^t E[R(\theta)]d\theta,$$

Consequently,

$$\begin{split} \frac{d}{dt}e^{bt}E[R(t)] &= \gamma e^{bt}E[I(t)], \\ e^{bt}E[R(t)] &= \gamma \int_0^t e^{b\theta}E[I(\theta)]d\theta, \\ e^{bt}E[R(t)] &\leq \gamma \int_0^t e^{b\theta}e^{-(b+\gamma-\beta)}I(0)d\theta, \\ E[R(t)] &\leq \frac{\gamma}{\beta-\gamma}[e^{(\beta-b-\gamma)t}-e^{-bt}]I(0). \end{split}$$

If  $\beta < b + \gamma$ , then

$$\lim_{t\to\infty} E[R(t)] = 0$$

Now S(t) + I(t) + R(t) = N, indicating that the population size remains constant

$$E[S(t)] + E[I(t)] + E[R(t)] = N$$

For analytical simplicity and to ensure a constant total

population, we assume equal birth and death rates, as commonly adopted in classical epidemic modeling frameworks.

Thus

$$\lim_{t\to\infty} E[S(t)] = N$$

Theorem 2.

Let S(t), I(t) and R(t) be the solutions of the fractional stochastic equations (2.1).

If  $R_0 < 1$ ,

Then:

$$\lim_{t \to \infty} E[S(t)] = N,$$

$$\lim_{t \to \infty} E[I(t)] = 0 , \lim_{t \to \infty} E[R(t)] = 0$$

Proof: consider the equation

$$v(t) = I(0) + \frac{1}{\Gamma(\alpha)} \int_0^t (t - \theta)^{\alpha - 1} (\beta - \gamma - b) v(\theta) d\theta + \frac{\sigma_2}{\Gamma(\alpha)} \int_0^t (t - \theta)^{\alpha - 1} v(\theta) dW(\theta),$$

$$E[v(t)] = I(0) + \frac{1}{\Gamma(\alpha)} \int_0^t (t - \theta)^{\alpha - 1} (\beta - \gamma) d\theta$$
$$- b) E[v(\theta)] d\theta$$

According to [21], we get

$$E[v(t)] = \int_0^\infty \xi_\alpha(\Theta) e^{(\beta - \gamma - b)t^\alpha \Theta} I(0) d\Theta$$

$$= \sum_{j=0}^{\infty} \frac{((\beta - \gamma - b)t^{\alpha})^j}{\Gamma(1 + \alpha j)} I(0)$$
 Mittage-Leffer function

Hence,

$$E[I(t)] \le E[v(t)] \to 0$$
as  $t \to \infty$ 

# 4. A Fractional Stochastic Epidemic Model Based on Fractional Brownian Motion

Fractional indicates the use of fractional-order stochastic processes, enabling the model to capture memory effects and long-range dependencies in epidemic dynamics, thus generalizing classical stochastic approaches.

To incorporate both long-memory effects and mean-reverting random fluctuations into epidemic dynamics, we extend the classical stochastic SIR model by introducing fractional Brownian motion and a fractional Ornstein–Uhlenbeck process.

Consider the following model:

$$dS(t) = \mu N - \mu S - W_{\alpha}^* SI + \gamma I ] dt - \sigma SIdW_{\alpha}(t),$$
  
$$dI(t) = [W_{\alpha}^* SI - \mu I - \gamma I] dt + \sigma SIdW_{\alpha}(t).$$

where  $W_{\alpha}(t)$  is the fractional Brownian motion, constructed by El-Borai and El-Nadi, see [2-9],  $\sigma$  is the standard deviation of the noise and  $W_{\alpha}^*(t)$  is the fractional Ornstein-Uhlenbeck process defined by

$$dW_{\alpha}^{*}(t) = \sigma_{3}(\beta - W_{\alpha}^{*}(t))dt + \sigma_{4}dW_{\alpha}(t),$$

This relation has been studied in [10],

Here  $\sigma_3 > 0$  is the speed of reversion,  $\sigma_4 > 0$  is the intensity of volatility.

Setting

$$v(t) = W_{\alpha}^*(t) - \beta,$$

we obtain

$$dv(t) = -\sigma_3 v(t) dt + \sigma_4 dW_{\alpha}(t),$$
  
$$v(0) = \beta_0 - \beta, \quad \beta_0 = W_{\alpha}^*(0).$$

The solution is given by

$$v(t) = e^{-t\sigma_3}(\beta_0 - \beta) + \sigma_4 \int_0^t e^{-(t-s)\sigma_3} dW_{\alpha}(s)$$

Hence.

$$W_{\alpha}^{*}(t) = \beta_0 + e^{-t\sigma_3}(\beta_0 - \beta) + \sigma_4 \int_0^t e^{-(t-s)\sigma_3} dW_{\alpha}(s).$$

The expectation of  $W_{\alpha}^{*}(t)$  is given by

$$E[W_\alpha^*(t)] = \beta_0 + e^{-t\sigma_3}(\beta_0 - \beta).$$

The variance of  $W_{\alpha}^{*}(t)$  is:

$$var[W_{\alpha}^{*}(t)] = \sigma_4^2 \int_0^t e^{-2(t-s)\sigma_3} \frac{s^{\alpha-1}}{\Gamma(\alpha)} ds.$$

Notice that at  $\alpha = 1$ ,

$$\begin{split} E[W_{\alpha}^{*}(t)] &= \beta_{0} + e^{-t\sigma_{3}}(\beta_{0} - \beta), \\ var[W_{\alpha}^{*}(t)] &= \frac{\sigma_{4}^{2}}{2\sigma_{3}}[1 - e^{-2t\sigma_{3}}]. \end{split}$$

We aim to find a deterministic function  $G(t, \alpha)$ , such that

$$\left[\int_0^t e^{-(t-s)\sigma_3} dW_\alpha(s)\right] dt = G(t,\alpha) dW_\alpha(t).$$

We notice that

$$\begin{split} \int_{0}^{t} & \left[ \int_{0}^{\eta} e^{-(\eta - s)\sigma_{3}} dW_{\alpha}(\eta) \right] d\eta = \int_{0}^{t} G(\eta, \alpha) \ dW_{\alpha}(\eta) = \\ & \frac{1}{\sigma_{3}} \int_{0}^{t} \left[ 1 - e^{-(t - s)\sigma_{3}} \right] \ dW_{\alpha}(s), \\ & \frac{1}{\sigma_{3}^{2}} E \left[ \left\{ \int_{0}^{t} \left[ 1 - e^{-(t - s)\sigma_{3}} \right] dW_{\alpha}(s) \right\} \right]^{2} \\ & = E \left[ \left\{ \int_{0}^{t} G(\eta, \alpha) \ dW_{\alpha}(s) \right\}^{2} \right] \\ & = \int_{0}^{t} G^{2}(\eta, \alpha) \frac{\eta^{\alpha - 1}}{\Gamma(\alpha)} d\eta \end{split}$$

Thus, we have

$$\frac{1}{\sigma_3^2} \int_0^t \left(1 - e^{-(t-s)\sigma_3}\right)^2 \frac{s^{\alpha-1}}{\Gamma(\alpha)} ds = \int_0^t G^2(s,\alpha) \frac{s^{\alpha-1}}{\Gamma(\alpha)} ds$$

Consequently, it follows that

$$\frac{t^{\alpha-1}G^2(t,\alpha)}{\Gamma(\alpha)} = \frac{2}{\sigma_3} \int_0^t \left[ e^{-(t-s)\sigma_3} - e^{-2(t-s)\sigma_3} \right] \frac{s^{\alpha-1}}{\Gamma(\alpha)} ds.$$

Hence, the stochastic process  $W_{\alpha}^{*}(t)$  can be expressed as:

$$W_{\alpha}^{*}(t)dt = [\beta + (\beta_0 - \beta)e^{-t\sigma_3}]dt + \sigma_4 G(t, \alpha) dW_{\alpha}(t).$$

Since given that S(t)+I(t)=N, it is sufficient to study the fractional stochastic equation for I(t):

$$dI(t) = [\{\beta + (\beta_0 - \beta)e^{-t\sigma_3}\}I(N - I) - I\mu - I\gamma]dt + \sigma_4\sigma I(N - I)dW_{\alpha}(t)$$
(4.1)

With the initial condition  $I(0) = I_0 \in (0, N)$ 

Theorem 3. For any given initial value  $I_0 \in (0, N)$ , the fractional stochastic differential equation (2) has a unique global positive solution  $I(t) \in (0, N)$  for all  $t \ge 0$ , with probability one,

$$P(I(t) \in (0,N), \forall t \geq 0) = 1$$

Proof: Consider the following fractional stochastic model:

$$du = \{\beta_0 + (\beta_0 - \beta)e^{-t\sigma_3}(N - e^u)\}du + \{-(\mu + \gamma)dt - \frac{1}{2}\sigma^2\sigma_4^2 \frac{t^{\alpha - 1}}{\Gamma(\alpha)}(N - e^u)^2\}dt$$
(4.2)

With the initial value  $u(0) = I_0$ 

It is clear that the coefficient of model 4.2 satisfies the local Lipschitz condition, thus there is a local solution u(t), of the model 4.2, see [21].

Therefore, it is easy to check that  $I(t) = e^{u(t)}$  is the positive solution of model 4.1 with the initial value  $I_0$ .

Although the current study emphasizes theoretical formulation and simulation, the proposed fractional stochastic model is well-suited for parameter estimation based on empirical data. The fractional order  $\alpha$  may be estimated through memory-sensitive residual minimization, generalized least squares, or optimization of model fit against cumulative case trajectories. The stochastic intensities  $\sigma_1$  and  $\sigma_2$  can be inferred via maximum likelihood estimation or Bayesian techniques. In particular, Markov Chain Monte Carlo (MCMC) methods are highly effective for capturing latent noise structures. Incorporating real-time epidemiological data would enable dynamic model calibration, support real-world forecasting, and inform data-driven public health decision-making [19-22].

Numerical simulation of Stochastic Differential Equations (SDEs) presents multiple computational challenges due to the closed-form solutions, the absence of stochastic characteristics of the system, and the high demands of convergence accuracy. Implicit schemes such as the backward Euler method offer strong convergence properties but require solving nonlinear equations at each time step, resulting in increased computational cost. Furthermore, Monte Carlo (MC) methods, which are widely used to approximate the expectation of functionals of SDE solutions, suffer from slow convergence rates of order  $O(N^{-1/2})$ , demanding a large number of samples to achieve desired accuracy. To address this, Multilevel Monte Carlo (MLMC) techniques have been developed to reduce total cost significantly while maintaining the same accuracy level. Other numerical methods for SDEs include the Euler-Maruyama method, Milstein method, and stochastic Runge-Kutta methods, each with trade-offs between accuracy, convergence, and computational efficiency

On the other hand, Fractional Differential Equations (FDEs) are characterized by memory effects and nonlocality, which introduce considerable computational burdens. Timefractional derivatives require storing the entire solution history, while space-fractional derivatives lead to nearly dense matrices. The computational complexity of fractional models typically scales worse than classical PDEs: for instance, time-fractional equations may reach O(N<sup>2</sup>M), and space-time fractional equations can grow as O(NM(M + N)), where N and M denote the number of time steps and grid points, respectively. Solving such models often necessitates specialized schemes such as the finite difference method (FDM) for fractional time and space derivatives, the finite element method (FEM) for irregular domains, spectral methods for high-accuracy needs, and fast Fourier transform (FFT)-based methods for reducing complexity. Additionally, short-memory principles and parallel computing are frequently used to alleviate memory and performance constraints [24].

In both cases, the selection of numerical methods must consider the trade-offs between stability, accuracy, computational cost, and the specific structure of the equations. The development and implementation of efficient algorithms remain an active area of research, especially in real-time simulation and data-driven forecasting contexts.

# 5. Application of the SIR Model in Epidemic Modeling

The proposed epidemic models were simulated using a discrete-time iterative scheme based on the explicit Euler method. At each step, the numbers of susceptible, infected, and recovered individuals were updated according to the governing equations, providing a clear and widely accepted approximation of the epidemic dynamics. Implementation was performed in Python (Anaconda environment) using standard scientific libraries, including NumPy, Pandas, and Matplotlib, ensuring reproducibility and clear visualization of the results.

In this section, we present numerical simulations to illustrate the behavior of the proposed fractional stochastic epidemic model. The aim is to demonstrate how different parameter values, particularly the basic reproduction number  $R_0$ , influence the epidemic dynamics over time.

To simulate the behavior of the epidemic model under various transmission scenarios, we used a deterministic SIR framework implemented in Python. The parameters  $\beta$  (transmission rate) and  $\gamma$  (recovery rate) were selected to achieve specific basic reproduction numbers  $(R_0)$ , reflecting different epidemic intensities. Initial conditions assume that 1% of the population is infected, with the remaining 99% susceptible. The total population is normalized to 1. Each simulation was run over a 60-day period to observe infection dynamics, and the impact of  $R_0$  values on peak infection levels and timing was assessed. The model does not incorporate real-world datasets but is designed to demonstrate theoretical behavior based on commonly accepted parameter ranges.

The simulations were implemented in Python using a deterministic SIR framework to analyze how different values of the transmission rate ( $\beta$ ) and recovery rate ( $\gamma$ ) influence the epidemic curve. By adjusting  $\beta$  and  $\gamma$ , we generated scenarios corresponding to various basic reproduction numbers ( $R_0$ ), including  $R_0 = 5$  (high),  $R_0 = 3$  (moderate), and  $R_0 = 1.5$  (low). These values were selected based on ranges reported in recent epidemiological literature. For instance, the basic reproduction number  $R_0$  for COVID-19 has been estimated to lie between 2.2 and 5.7 in early pandemic assessments, according to public health reports and modeling studies [25].

Rather than calibrating the model to real-world data, the objective of this simulation was to explore the qualitative behavior of the system under plausible epidemic conditions. This approach highlights the flexibility of the model and its ability to reflect key transmission dynamics without relying on specific datasets.

Let S=y[0] denote the number of individuals not yet infected, I=y[1] the number of individuals infected, R=y[2] the number of individuals recovered or died from the disease,  $\beta=0.6$  is the infected rate and  $\gamma=0.025$  is the recovery rate.

**Figure 1** presents the results of a simulation with parameters  $\beta = 0.6$  and  $\gamma = 0.025$ . The simulation illustrates a typical epidemic trajectory in which the susceptible population decreases over time, the number of infected individuals rises

and subsequently declines, and the recovered population steadily increases. This experiment is provided for illustrative purposes and is not based on empirical data.

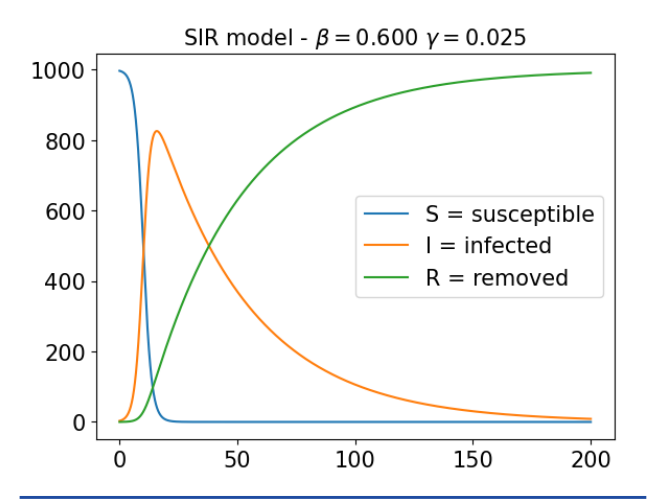


**Figure 1.** Simulation of the SIR Epidemic Model with Transmission Rate ( $\beta$ =0.6) and Recovery Rate ( $\gamma$ =0.025).

As shown in **Figure 2**, increasing the transmission rate  $\beta$  leads to a sharper and earlier peak in the number of infected individuals, while lower values of  $\beta$  help flatten the curve and spread the infections over a longer period.

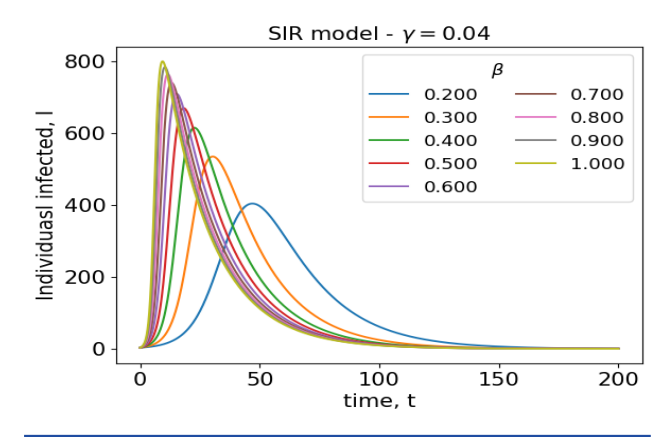


**Figure 2.** Effect of Varying Transmission Rate  $(\beta=0.2,0.03,...,1.0)$  on the Number of Infected Individuals Over Time in the SIR Model with  $\gamma=0.04$ .

The framework separates the population into categories using the standard SIR notation defined in Section 2, where S(t), I(t) and R(t) denote the susceptible, infected, and recovered populations, respectively. A major assumption is that recovered individuals acquire immunity to the disease.

We consider the total population N to be normalized to 1. The initial state for the infectious category  $I_0$  is the proportion of the total population infected at time  $T_0$ . The initial state for the susceptible population  $S_0$  is the remaining population  $N-I_0$ , assuming no vaccination. It is also believed that there is no individual found at the start. The model also assumes that the population remains constant, meaning that there are no additional births or deaths due to causes other than the pandemic.

The epidemic initiates when susceptible individuals encounter infectious individuals, leading to new infections over time. The number of new infections is proportional to both the susceptible and infectious populations, calculated as New infection =  $\beta SI$ -> (I), where  $\beta$  represents the transmission rate. New recoveries occur as a subset of the infectious population either recovers or dies. The number of recoveries is given by = New recovery =  $\gamma I$  -> (II), where  $\gamma$  is the recovery rate.

The effects of new infections and recoveries on the *S*, *I* and *R* compartments are described as follows:

The susceptible population (S) decreases as new infections occur:

S[T+1] = S[T] - new infections. [T]

The infectious population grows with new infections and declines with new recoveries:

I[T+1] = I[T] plus new infections. [T] - New Recovery.

The recovered population grows as new recoveries occur.

$$R[T+1] = R[T] + New Recovery$$

An infection is considered an epidemic when it spreads over time, the number of new infections exceeds the number of new recoveries.

New infections lead to new recoveries ( $\beta SI > \gamma I$ ), as seen in (I) and (II).

The effective reproductive number is defined as  $\frac{S\beta}{\gamma} > 1$ .

At the start of an epidemic, almost the entire population is vulnerable, resulting in  $S = S_0 = 1$ .

Reproduction number  $=\frac{\beta}{\gamma}$ , often known as the fundamental reproduction number  $(R_0)$ .

If  $R_0 > 1$ , the infection becomes an epidemic; otherwise, it dies off.

#### 5.1. SIR Model for $R_0 = 5$

The basic reproduction number  $R_0$  for Covid-19 is estimated to range between 2.2 to 5.7. We consider a scenario where  $R_0$  is 5 and the initial state of infectious population is 1%. We use  $\beta=0.75$  and  $\gamma=0.15$  to obtain the desired  $R_0$  of 5.0 [25]. These simulations use a basic reproduction number  $R_0=5$  to reflect high transmissibility scenarios, consistent with early estimates COVID-19, which replaced  $R_0$  between 2.2 and 5.7. A key model-based study reported a central estimate of  $R_0{\approx}5.7$ , highlighting the virus's potential for rapid spread in the absence of control measures.

In the simulation with  $R_0 = 5$ , shown in **Figure 3**, the infection peaks rapidly, reaching over 52% of the population around day 12. The epidemic infects nearly the entire population by the end of the simulation.

## 5.2. SIR Model for $R_0=3$

To demonstrate the impact of reduced transmissibility, a hypothetical scenario is considered in which the basic reproduction number is set to  $R_0 = 3$ . Since  $R_0 = \frac{\beta}{\gamma}$ , this reduction can theoretically be achieved by decreasing the transmission rate  $\beta$ , increasing the recovery rate  $\gamma$ , or applying both adjustments. In this scenario,  $\beta$  is set to 0.45 while  $\gamma$  remains at 0.15, producing a resulting  $R_0$  to 3.

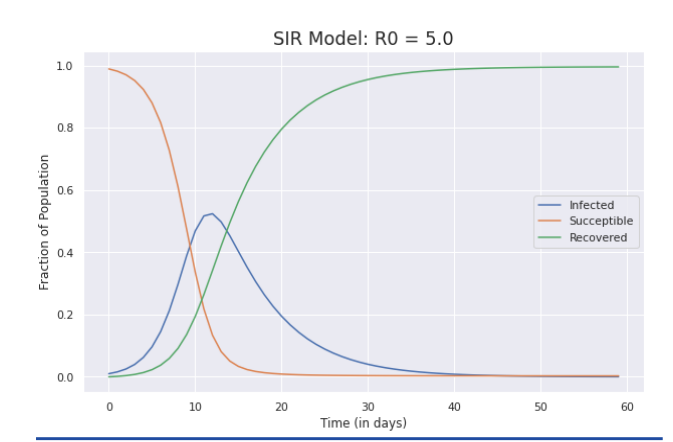


**Figure 3**. Maximum Infectious population at a time: 52.43%, total Infected population: 99.6%.

In **Figure 4**, with  $R_0$  reduced to 3 by decreasing  $\beta$  to 0.45 while maintaining  $\gamma$  at 0.15, the infection curve exhibits a substantially reduced peak of infections. The peak proportion of infectious individuals falls to 32.22%, occurring around day 20, thereby providing additional time for potential intervention measures.

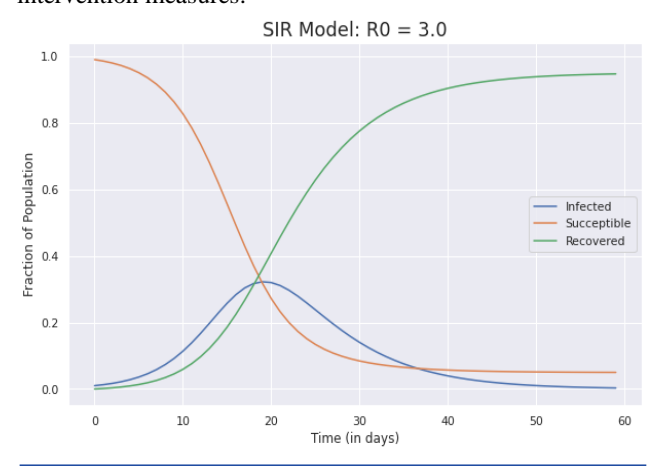


**Figure 4**. Maximum Infectious population at a time :32.22%, total Infected population :95.01%.

This results in a decrease from approximately 52% in the previous scenario with  $R_0 = 5$ , to 32.22%, and nearly 5% of the total population remains uninfected by the end of the epidemic.

#### **5.3. SIR Model for** $R_0$ **=1.5**

To demonstrate the impact of reduced transmissibility, a hypothetical scenario is considered in which the basic reproduction number is set to  $R_0=1.5$ . Since  $R_0=\beta/\gamma$ , this reduction can be achieved by adjusting either the transmission rate  $\beta$  or the recovery rate  $\gamma$ . In this case,  $\gamma$  is increased to 0.3 while  $\beta$  remains unchanged, yielding a resulting  $R_0$  of 1.5.

In **Figure 5**, this reduction markedly attenuates the epidemic dynamics. The peak proportion of infectious individuals decreases to 7.28%, occurring around day 25, while the cumulative number of infections is restricted to approximately 60% of the total population.

#### **Article**



**Figure 5**. Maximum Infectious population at a time: 7.28%, total Infected population: 60.07%.

#### 5.4. Flatten the curve

The concept of flattening the curve effectively captures the epidemic dynamics described above. Reducing  $R_0$  decreases both the transmission potential and the peak prevalence of infections, while also postponing the infection peak, providing additional time for effective intervention strategies. The following analysis examines how the peak level and the overall extent of infection vary with different values of  $R_0$ .

**Figure 6** shows the effect of reducing  $R_0$  from 6 to 2, which delays the epidemic peak by more than two weeks and decreases the maximum proportion of infections, thereby mitigating the burden on healthcare systems.

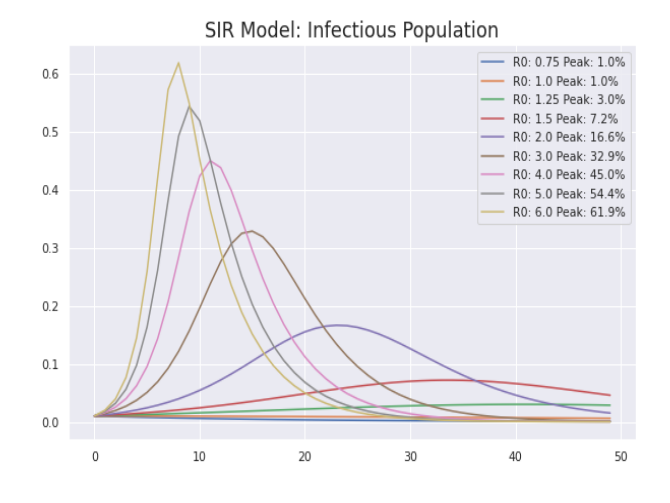
As  $R_0$  drops, the curve for infectious population flattens. When  $R_0$  is 6, more than 60% of the population becomes infected by the eighth day, whereas when  $R_0$  is 2, the highest infectious population is 16.7% by the twenty-fourth day. That means a reduction in  $R_0$  from 6 to 2 provides us an extra two weeks to prepare for the peak infection. It is also worth noting that when  $R_0$  falls, so does the degree of infection. When  $R_0$ =6, the entire population becomes infected, however when  $R_0$ =2, 20% of the population remains uninfected after the epidemic has ended.

As  $R_0$  decreases, the infection curve flattens. For  $R_0 = 6$ , more than 60% of the population becomes infected by the eighth day, whereas for  $R_0 = 2$ , the peak proportion of infectious individuals is 16.7% on the twenty-fourth day. Reducing  $R_0$  from 6 to 2 effectively extends the time to peak infection by approximately two weeks, providing additional time for preparedness. Importantly, the model further indicates that lower values of  $R_0$  reduce the overall extent of infection: while nearly the entire population becomes infected when  $R_0 = 6$ , about 20% of the population remains uninfected when  $R_0 = 2$ .

The COVID-19 pandemic demonstrated that elevated transmission rates can rapidly overwhelm healthcare capacity, defined as the point where patient demand exceeds available hospital resources. To capture these dynamics, a fractional SIR model with the Mittag—Leffler kernel was introduced in [12], reflecting memory effects and nonlocal behavior. Experiences from countries such as Italy and Spain highlighted how sudden surges can deplete ICU capacity and essential medical supplies. The proposed fractional stochastic epidemic model can be extended to incorporate public health interventions such as vaccination programs and behavioral mitigation strategies. Specifically, vaccination can be modeled by introducing a time-dependent control term that adjusts the susceptible or recovered compartments according to immunization rates.

Additionally, behavioral responses can be reflected by allowing the transmission coefficient  $\beta(t)$  to vary over time, potentially influenced by policy enforcement, public compliance, or seasonal effects. In stochastic formulations, such time-varying parameters may also be subject to random fluctuations, modeled through additional noise-driven terms. These theoretical extensions highlight the model's structural flexibility and its potential relevance for future applications involving real-time intervention strategies under uncertainty.

Although the current formulation considers a constant transmission rate  $\beta$ , it can be extended to  $\beta(t)$  to account for time-dependent interventions or seasonal variations, which can be explored in future studies.



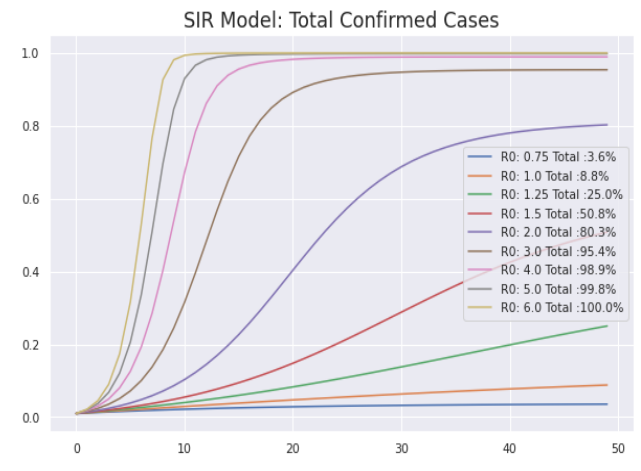


Figure 6. Effect of Ro on Infectious Population and Total Confirmed Cases in the SIR Model.

#### 6. Conclusion

This study examined a stochastic fractional epidemic model incorporating a recently proposed formulation of the fractional Wiener process. The analysis addressed the existence, uniqueness, and qualitative behavior of solutions within a generalized stochastic framework. Additionally, a model driven by a formulation of fractional Brownian motion was considered, demonstrating the impact of memory and long-range dependence in the modeling of disease transmission under uncertainty.

# References

- [1] Ul Haq, I.; Ali, N.; Bariq, A.; Akgül, A.; Baleanu, D.; Bayram, M. Mathematical modelling of COVID-19 outbreak using Caputo fractional derivative: Stability analysis. Appl. Math. Sci. Eng. 2024, 32 (1), 2326982.
- [2] Prather, R. On a Stochastic Model of Epidemics; Master's Thesis, University of Southern Mississippi: Hattiesburg, MS, USA, 2021.
- [3] El-Nadi, K. E.-S. Asymptotic formulas for some cylindrical functions. Uspekhi Mat. Nauk 1969, 24 (3), 143–147.
- [4] El-Nadi, K. E.-S. Asymptotic methods in difference differential equations and its applications. Arab J. Numer. Anal. 1970, 9 (4), 873–883.
- [5] Montroll, E.W.; Shlesinger, M.F. On the Wonderful World of Random Walks. In: Lebovitz, J., Montroll, E., Eds.; Studies in Statistical Mechanics, Vol. 11; North-Holland: Amsterdam, 1984; p. 1–121.
- [6] El-Nadi, K. E.-S. On some boundary-value problems in queuing theory. Syst. Control Lett. 1983, 2 (5), 307–312.
- [7] El-Borai, M. M.; El-Nadi, K. E.-S. On the Construction of a New Fractional Brownian Motion. Math. Comput. Sci.: Contemp. Dev. 2024, 9, 52–60.
- [8] El-Nadi, K. E.-S. On some stochastic models of cancer. Can. J. Biomed. Eng. Technol. 2010, 1, 42049
- [9] El-Nadi, K. E.-S. On some stochastic differential equations and fractional Brownian motion. Int. J. Pure Appl. Math. 2005, 24(3), 415–423.
- [10] Wang, W.; Cai, Y.; Ding, Z.; Gui, Z. A stochastic differential equation SIS epidemic model incorporating Ornstein–Uhlenbeck process. Physica A: Stat. Mech. Appl. 2018, 509, 921–936.
- [11] Nisar, K.S.; Farman, M.; Abdel-Aty, M.; Cao, J. A review on epidemic models in sight of fractional calculus. Alex. Eng. J. 2023, 75, 81–113.
- [12] Atangana, A.; Araz, S.İ. Fractional Stochastic Differential Equations: Applications to Covid-19 Modeling, First ed.; Springer, Singapore, 2022.
- [13] Akinlar, M.A.; Inc, M.; Gómez-Aguilar, J.F.; Boutarfa, B. Solutions of a disease model with fractional white noise. Chaos Solitons Fract. 2020, 137, 109840.
- [14] Gourieroux, C.; Lu, Y. SIR model with stochastic transmission. arXiv:2011.07816, 2020.

- [15] Alkahtani, B. S. T.; Koca, I. Fractional stochastic SIR model. Results Phys. 2021, 24, 104124.
- [16] Nie, N.; Jiang, J.; Feng, Y. Parameter Estimation for a Class of Fractional Stochastic SIRD Models with Random Perturbations. Fund. J. Math. Appl. 2023, 6 (2), 101–106.
- [17] El-Nadi, K.E.-S. Asymptotic methods and some difference fractional differential equations. Int. J. Contemp. Math. Sci. 2006, 1 (1), 3–13.
- [18] El-Borai, M. M. Some probability densities and fundamental solutions of fractional evolution equations. Chaos Solitons Fract. 2002, 14 (3), 433–440.
- [19] Demiris, N. Bayesian inference for stochastic epidemic models using Markov chain Monte Carlo methods; PhD Thesis, University of Nottingham: Nottingham, UK, 2004.
- [20] Nshimiyimana, P. Stochastic epidemic models; Master's Thesis, University of Chicago: Chicago, USA, 2017.
- [21] El-Borai, M.M.; El-Nadi, K.E.-S. On Some Stochastic Parabolic Systems Driven by New Fractional Brownian Motions. Asian J. Probab. Stat. 2024, 26(9), 1–8.
- [22] Kypraios, T.; Neal, P.; Prangle, D. A tutorial introduction to Bayesian inference for stochastic epidemic models using Approximate Bayesian Computation. Math. Biosci. 2017, 287, 42–53.
- [23] Wang, L. Numerical Solutions of Stochastic Differential Equations; PhD Thesis, University of Tennessee: Knoxville, USA, 2016.
- [24] Gong, C.; Bao, W.; Tang, G.; Jiang, Y.; Liu, J. Computational challenge of fractional differential equations and the potential solutions: a survey. Math. Probl. Eng. 2015, 258265.
- [25] Sanche, S.; Lin, Y. T.; Xu, C.; Romero-Severson, E.; Hengartner, N.; Ke, R. High contagiousness and rapid spread of severe acute respiratory syndrome coronavirus 2. Emerg. Infect. Dis. 2020, 26 (7), 1470–1477.